ELSEVIER
SAUNDERS

Neurosurg Clin N Am 16 (2005) 115–134

NEUROSURGERY
CLINICS
OF NORTH AMERICA

# Diffusion tensor magnetic resonance imaging of brain tumors

L. Celso Hygino Cruz, Jr, MD[a], A. Gregory Sorensen, MD[b,*]

[a]*Clínica de Diagnóstico por Imagem, Multi-Imagem Ressonância Magnética, Av. das Ameréricas 4666, Centro Médico Barrashopping, Rio de Janeiro, Brazil*

[b]*Department of Radiology, Massachusetts General Hospital, Athinoula A. Martinos Center for Biomedical Imaging, Division of Health Sciences and Technology, Haravrd-MIT, Building 149m 13th Street, Boston, MA 02421, USA*

Primary neoplasms of the central nervous system (CNS) have a prevalence between 15,000 and 17,000 new cases annually in the United States, and when metastatic lesions are included, brain tumors are estimated to cause the deaths of 90,000 patients every year [1,2]. Gliomas remain the most common primary CNS tumor, accounting for 40% to 50% of cases [3] and 2% to 3% of all cancers [4]. Despite new techniques of treatment, patient survival still remains low, varying between 16 and 53 weeks [5].

For more than 40 years [6], nuclear magnetic resonance has been used to analyze and assess brain tumors. It is generally accepted that conventional MRI, typically T1- and T2-weighted imaging, tends to underestimate the extent of the tumor, which can, in turn, lead to suboptimal treatment [7]. New functional MRI (fMRI) sequences, such as diffusion imaging, perfusion imaging, and spectroscopic imaging, have been widely used to evaluate such tumors. In this review, diffusion tensor imaging (DTI), one of the newer methods, is described, particularly the ability of DTI to aid in differentiating a tumor from surrounding edema and infiltrating tumor [8] and, to some extent, to grade brain tumors [9].

## Diffusion MRI

### *Physical basis*

The random or Brownian movement of water molecules is the basis of diffusion. In the brain, the presence of tissue structures restricts free water motion [10–12], for example, rendering the diffusion of water molecules higher in the ventricles than in the parenchyma. MRI makes it possible to estimate the diffusivity of water molecules.

Because some pathologic processes seem to change the characteristic of the brain diffusion [13], diffusion-weighted imaging (DWI) has become increasingly popular over the past few years. In typical clinical practice, diffusion imaging is used to assess acute cerebral ischemia [14–17], where the water mobility acutely decreases after the onset of ischemia. The mechanisms to explain the decrease in diffusion coefficients are still controversial. Failure of the $Na^+/K^+$ adenosine triphosphatase pump is believed to play an important role in this process, however, leading many to term this state as *cytotoxic edema* [17,18]. Diffusion imaging has also been successfully applied to the evaluation of other neurologic conditions, such as multiple sclerosis [19–22], encephalitis [23], and Creutzfeldt-Jakob disease [24].

Most diffusion measurements today are made using a variant of the diffusion-weighted sequence first described by Stejskal and Tanner [25]. Their initial approach described a spin echo (SE) sequence together with two equal and opposite extra gradient pulses [25]; the amount of signal loss can be related to the magnitude of diffusion. For practical purposes, an echo planar imaging (EPI), SE, T2-weighted sequence is used, causing reduction of motion artifacts and speeding the time of acquisition [26]. Stejskjal and Tanner's [25] approach uses two magnetic pulses or gradients to label the spins: the application of the first diffusion gradient causes a dephasing of water protons;

* Corresponding author.
*E-mail address:* sorensen@nmr.mgh.harvard.edu (A.G. Sorensen).

1042-3680/05/$ - see front matter 
doi:10.1016/j.nec.2004.07.007

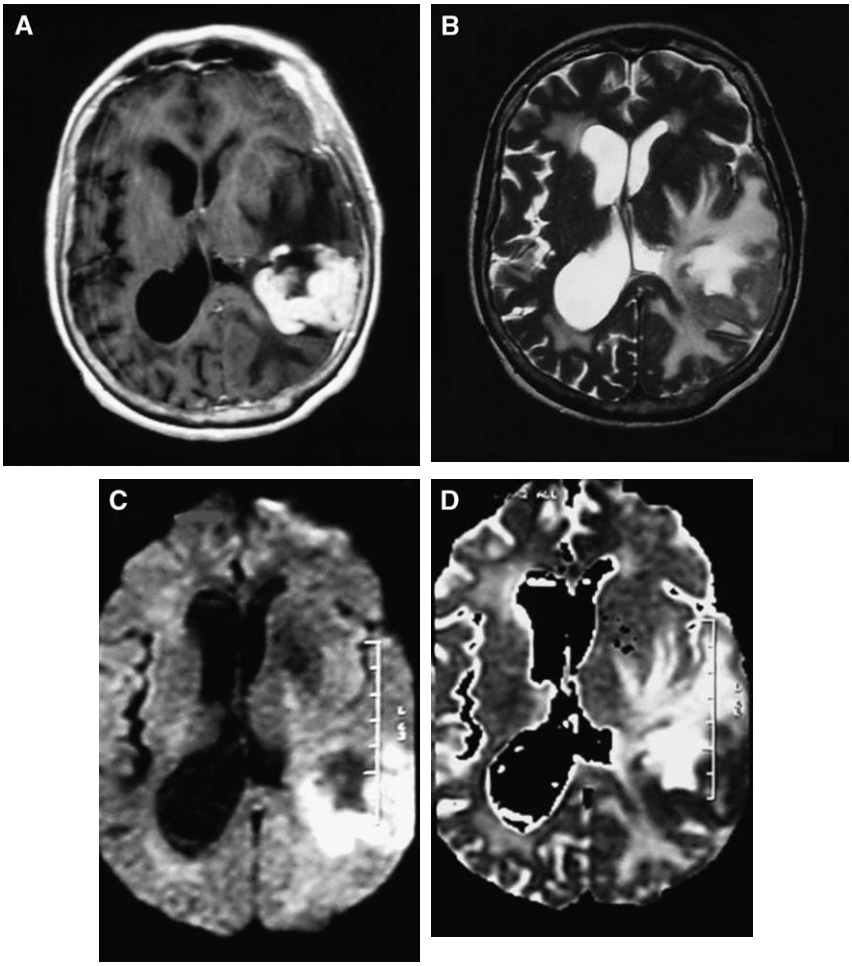


Fig. 1. A 75-year-old woman with a glioblastoma multiforme. (*A*) Contrast-enhanced, axial, T1-weighted image shows an enhancing necrotic mass surrounded by an abnormal hyperintense area on the axial T2-weighted image (T2WI). (*B*) These abnormal hyperintense T2WI areas can represent peritumoral edema or infiltrating tumor. The tumor is isohypointense on the T2WI, indicating high cellularity; this is also demonstrated as restricted diffusion on the diffusion-weighted image (*C*) and apparent diffusion coefficient map (*D*).

because they move randomly, not all water protons are in place for rephrasing from the application of the second diffusion gradient. Thus, there is a signal decrease that depends on how far the water molecules move [13]. The net signal on the final diffusion-weighted image is therefore influenced by the T2 tissue effect and by the tissue diffusion characteristics. By acquiring an image with little diffusion weighting and another image with substantial diffusion weighting, the apparent diffusion coefficient (ADC) can be calculated on a voxel-by-voxel basis, allowing the generation of a map that reflects solely the diffusion influence, excluding the T2 effects, which prevents misinterpretation from the so-called "T2 shine-through" effect [13,26].

### *Diffusion-weighted MRI in brain tumors*

Although most of this review focuses on DTI, a few words about the more common, nontensor (or "trace-weighted") DWI approaches are appropriate. DWI has been used to assess brain tumors, and although it has had limited success as a definitive prognostic tool, its proponents suggest that in certain settings, it can increase the sensitivity and specificity of MRI in the evaluation of brain tumors by providing information about

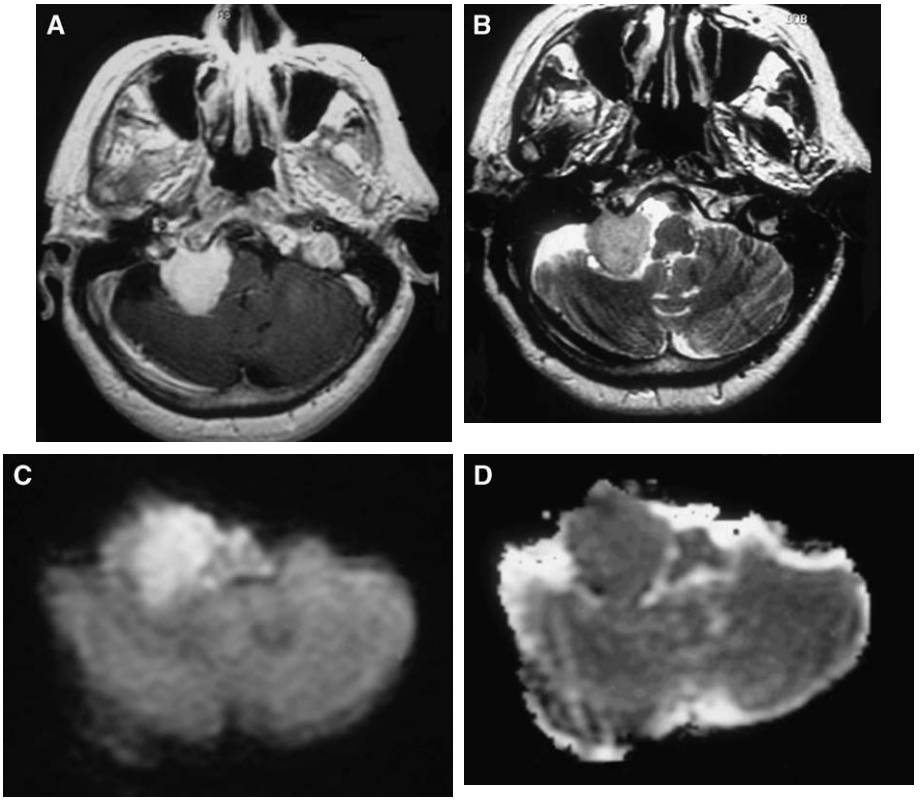


Fig. 2. An 84-year-old woman with a meningioma. An axial, postcontrast-enhanced, T1-weighted image (*A*) and an axial T2-weighted image (*B*) show an extra-axial enhancing lesion in the right cerebellopontomedullary angle cistern. Axial diffusion-weighted imaging (*C*) shows "T2-shine through," whereas the apparent diffusion coefficient map (*D*) demonstrates isointense signal intensity suggesting cellularity similar to that of brain tissue.

tumor cellularity, which may, in turn, improve prediction of tumor grade. Some also suggest that DWI can provide information about peritumoral neoplastic cell infiltration [8,9,27–31].

One example of a specific helpful arena in which DWI may be helpful is the distinction between brain abscesses and necrotic and cystic neoplasms on MRI. DWI can provide a sensitive and specific method for differentiating tumor from abscess in certain settings [32–35]. The abscesses have a high signal on DWI and a reduced ADC within the cavity. This restricted diffusion is thought to be related to the characteristic of the pus in the cavity. Because pus is a viscous fluid that consists of inflammatory cells, debris, and macromolecules like fibrinogen [36], this may, in turn, lead to reduced water mobility, lower ADC, and bright signal on DWI. Conversely, necrotic and cystic tumors display a low signal on DWI (similar to the cerebrospinal fluid [CSF] in the ventricles), with an increased ADC as well as isointense or hypointense DWI signal intensity in the lesion margins [34]. Although these findings can be helpful, they are, of course, not absolute; under certain conditions, restricted diffusion has been documented in hemorrhagic metastases, radiation necrosis, and cystic astrocytoma [37].

DWI is also an effective way of differentiating an arachnoid cyst from epidermoid tumors [38]. Both lesions present the same T1 and T2 signal intensity characteristic of CSF. On DWI, epidermoid tumors are hyperintense, because they are solidly composed, whereas arachnoid cysts are hypointense, demonstrating high diffusivity [38]. The ADC values of epidermoid tumors are similar to those of the brain parenchyma, whereas the ADC values of arachnoid cysts are similar to those of CSF [39]. As a result, DWI can be used to assess follow-up of surgically resected epidermoid tumors, proving efficacious in the detection of residual lesions [40].

Another use for DWI has been to attempt to assist in determination of the margins of tumors in

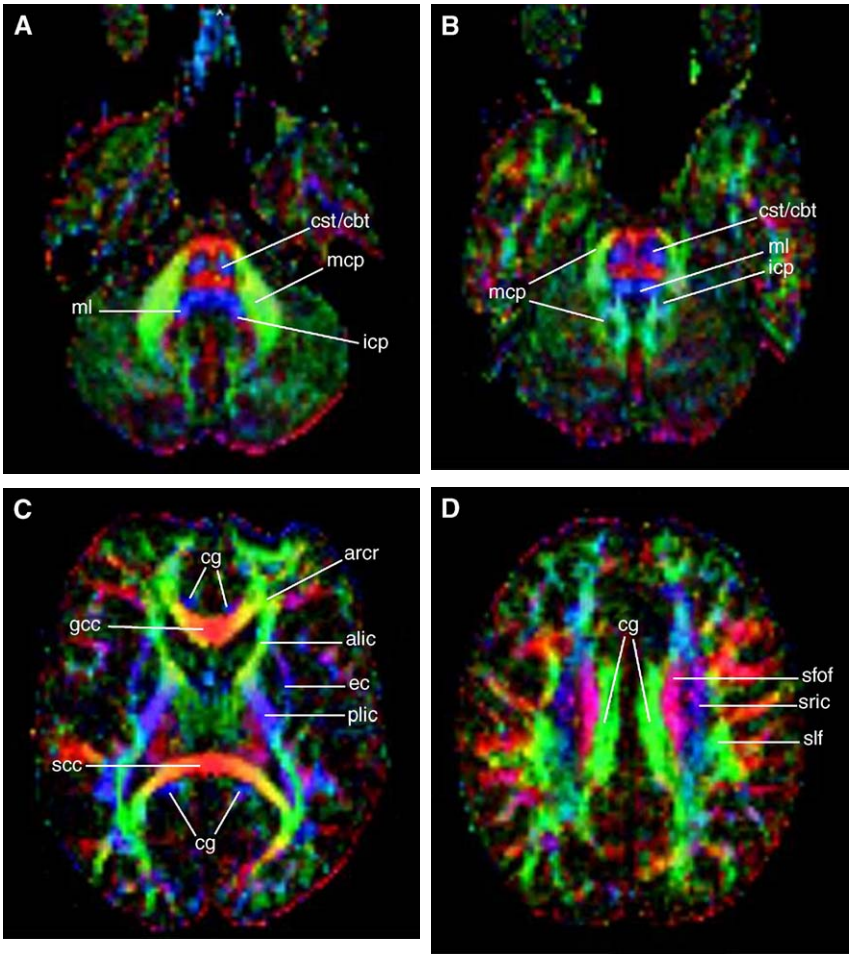


Fig. 3. Diffusion tensor imaging color-coded map of a healthy volunteer. Locations of white matter tracts are assigned on color maps. The direction of the main fiber tracts is represented by red (right-left), green-yellow (anterior-posterior), and blue (superior-inferior). Several main fiber tracts visible on color maps are annotated on the basis of anatomic knowledge. (*A–D*) Axial fractional anisotropic (FA) color maps. (*E–H*) Coronal FA color maps. (*I, J*) Sagittal FA color maps. Mcp, middle cerebral peduncle; cst, corticospinal tract; cbt, corticobulbar tract; ml, medial lemniscus; icp, inferior cerebellar peduncle; cg, cingulum; cc, corpus callosum; gcc, genu of corpus callosum; scc, splenium of corpus callosum; arcr, anterior region of corona radiata; alic, anterior limb of internal capsule; plic, posterior limb of internal capsule; ec, external capsule; sric, superior region of internal capsule; sfof, superior fronto-occipital fasciculus; ifof, inferior fronto-occipital fasciculus; slf, superior longitudinal fasciculus; ilf, inferior longitudinal fasciculus.

the brain. High-grade tumors tend to spread diffusely across the brain, moving along the fiber tracts [41,42]. Some studies have demonstrated the capability of DWI to discriminate the tumor, the infiltrating tumor, the peritumoral edema, and the normal brain parenchyma [8,9,14,43]. Other studies did not find any advantages of this method with regard to the evaluation of tumor extensions [44–46], however, likely because of the difficulty of finding any border even on histopathologic examination of some tumors.

Perhaps most helpfully, DWI has been shown to assist in assessing the cellularity of tumors [44]. In some studies, high-grade tumors have been found to have low ADC values (Fig. 1). This suggests a correlation between the ADC values and tumor cellularity [46,47], with lower ADC values suggesting high-grade lesions [46,48]. In some studies, however, ADC values found in high- and low-grade gliomas have overlapped somewhat [46]. Lymphoma, a highly cellular tumor, has hyperintensity on DWI and reduced ADC values [49],

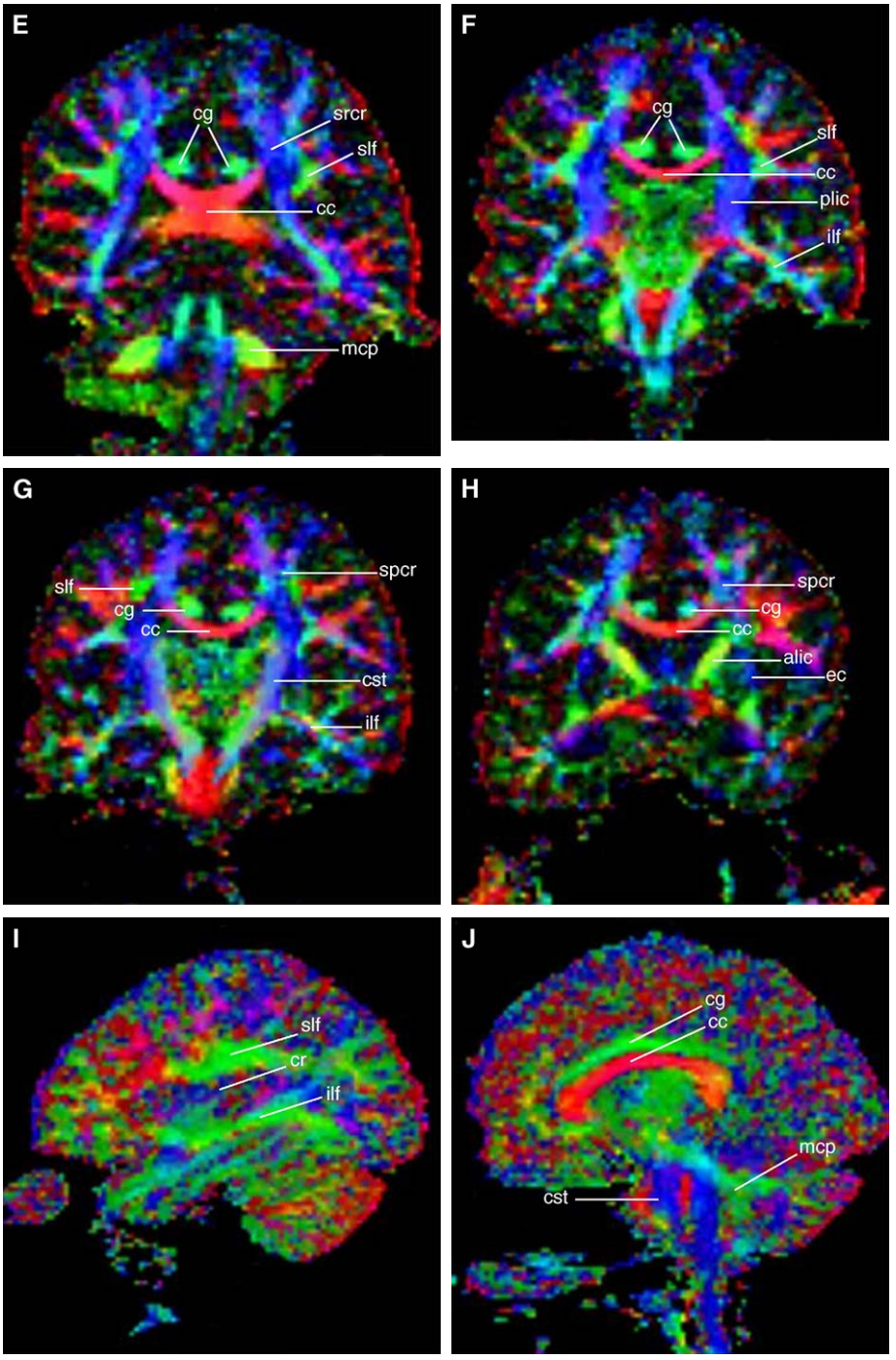


Fig. 3 (*continued*)

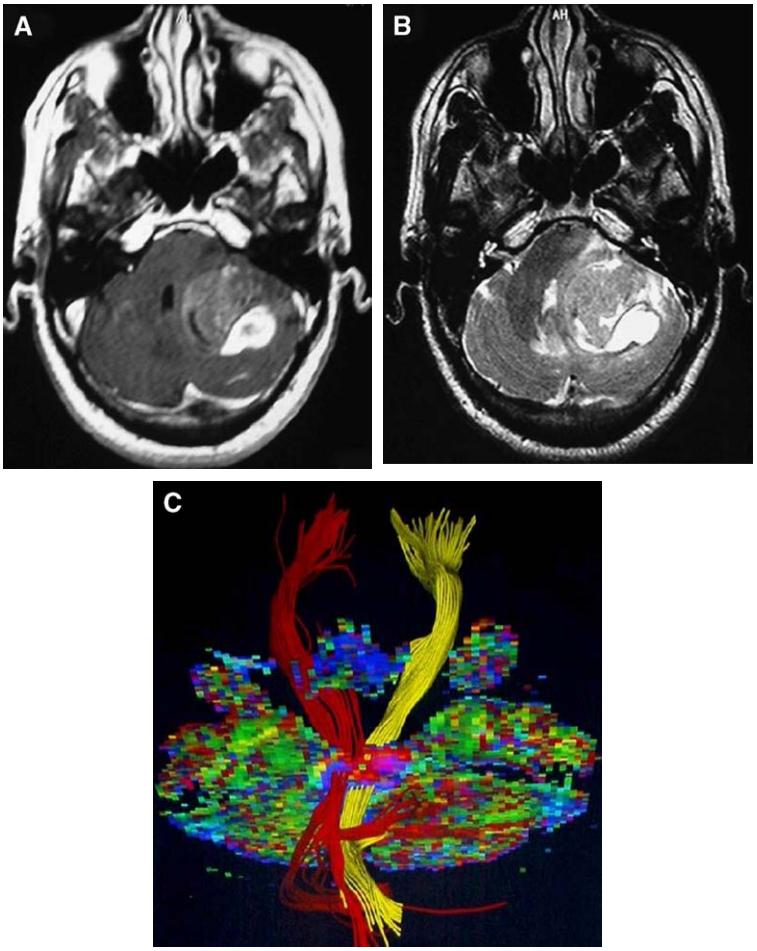


Fig. 4. A 47-year-old man with medulloblastoma. A heterogeneous mass with intratumoral hemorrhage (*A*) surrounded by peritumoral vasogenic edema (*B*) is located in the right cerebellum hemisphere. This mass causes compression and distortion of the fourth ventricle. (*C*) Tractography demonstrates contralateral displacement of the corticospinal tract without clear evidence of invasion or disruption of these fibers.

and it may be in differentiating lymphoma from other CNS lesions that DWI has its greatest value. Although meningiomas also have a restricted diffusion, displaying low ADC values (Fig. 2) [46], they rarely present difficulty in diagnosis. Metastases with perilesional edema have higher ADC values than a primary brain tumor with peritumoral edema, and some have suggested that this may allow better differentiation [28].

Finally, DWI may be useful for posttreatment assessment, demonstrating acute postoperative procedure–induced changes [50] but, more importantly, possibly providing an early surrogate marker for the efficacy of the chemotherapeutic treatment [51,52], because such treatments may cause cytotoxic or vasogenic edema that DWI can differentiate and monitor. DWI also has been suggested as a tool for monitoring the effectiveness of radiation therapy [2] In summary, DWI has a limited prognostic role but may become an important tool in assessing the response to radiation therapy and chemotherapy [2] as well as the complications related to each type of therapy [53,54].

## Diffusion tensor MRI

### *Physical basis*

The movement of water occurs in all three directions and is assumed to behave in a manner that physicists can describe using a Gaussian

approximation. When water molecules diffuse equally in all directions, this is termed *isotropic diffusion*. This phenomenon is typical in the ventricles, and at the resolution of standard MRI, also seems to be the case in the gray matter. In the white matter, however, free water molecules diffuse anisotropically, that is, the water diffusion is not equal in all three orthogonal directions [55,56,61]. This is likely because tissue structures cause impediment of the water motion; these structures likely include the cell membranes but, more importantly, the myelin sheath surrounding myelinated white matter [57]. Put another way, isotropic diffusion can be graphically represented as a sphere [58], whereas anisotropic diffusion can be graphically expressed as an ellipsoid [58], with water molecules moving farther along the long axis of a fiber bundle and less movement perpendicularly [59].

To estimate the nine tensor matrix elements required for a Gaussian description of water mobility, the diffusion gradient must be applied to at least six noncollinear directions (only six of the nine elements are unique under this assumption) [60]. The eigenvalues represent the three principal diffusion coefficients measured along the three coordinate directions of the ellipsoid [59]. The eigenvectors represent the directions of the tensor [60]. Because interpreting a tensor representation can be difficult, scalar metrics have been proposed to simplify DTI data [57]. For example, fractional anisotropy (FA) measures the fraction of the total magnitude of diffusion anisotropy. FA values vary from complete isotropic diffusion (graded as 0) up to complete anisotropic diffusion (graded as 1) [57,58].

In addition to assessment of the diffusion in a single voxel, DTI has been used to attempt to map the white matter fiber tracts. This is typically done by connecting a given voxel to the appropriately adjacent voxel in accordance with the direction that the voxel's principal eigenvector is oriented [62,63]. A color-coded map of fiber orientation can also be determined by DTI [64]. A different color has been attributed to represent a different fiber orientation along the three orthogonal spatial axes: in the standard convention, red stands for the left-to-right direction of x-oriented fibers, blue stands for the superior-to-inferior direction of y-oriented fibers, and green stands for the anterior-to-posterior direction of z-oriented fibers (Fig. 3) [64,65].

## Diffusion tensor MRI in brain tumors

Often, a primary aim of surgical brain tumor treatment is complete lesion resection without harming vital brain functions [66,67]. Because it is generally accepted that conventional MRI underestimates the real extent of the brain tumor, given its ability to verify neoplastic cells that infiltrate peritumoral areas of abnormal T2-weighted signal intensity [68], many practitioners are uncomfortable using only conventional MRI

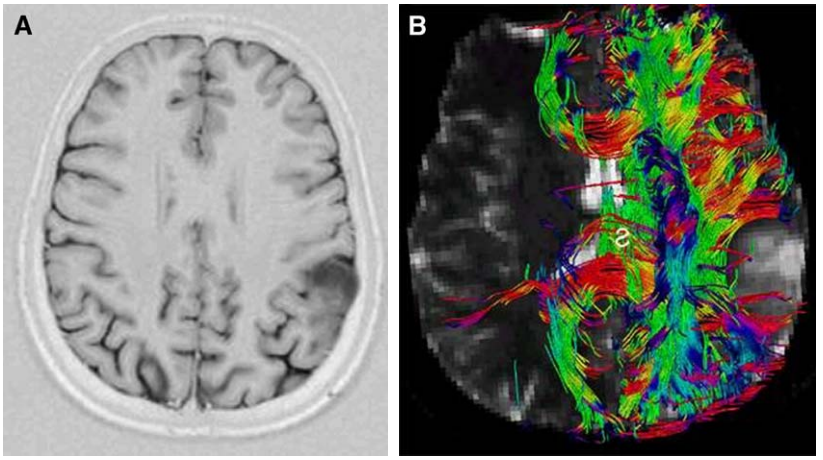


Fig. 5. A 42-year-old man with a diagnosis of a low-grade astrocytoma presented with early onset of focal seizures. (*A*) The MRI examination demonstrates an expansive lesion in the perirolandic area, which does not have hyperperfusion. (*B*) The mass lesion causes displacement of the main fiber tracts adjacent to the tumor, which is well demonstrated on tractography. There seems to be no invasion or disruption of these tracts.

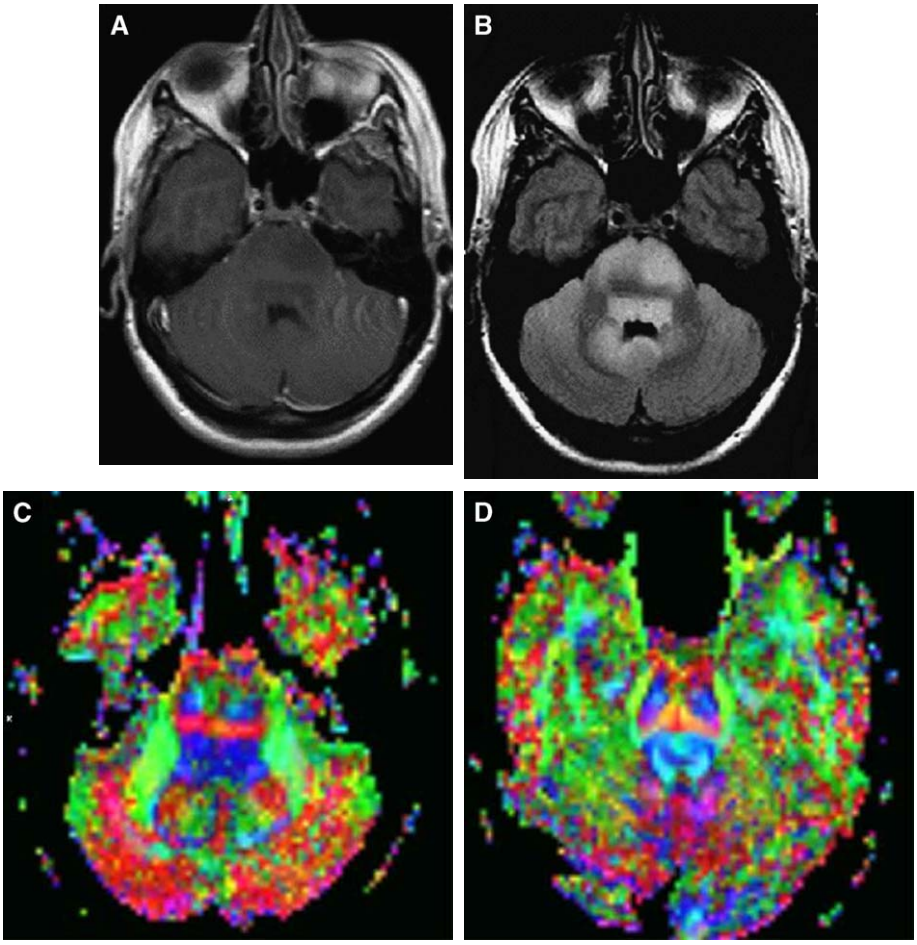


Fig. 6. An invading brain stem lesion that extends to the right cerebellum hemisphere though the middle cerebellar peduncle in a 40-year-old man who presented with left sixth cranial nerve palsy. The diagnosis of gliomatosis cerebri was made after a biopsy. The lesion does not enhance on the postcontrast T1-weighted image (*A*), has hyperintense signal on the T2-weighted image (*B*), and causes minimum expansion of the brain stem. Magnetic resonance spectroscopy shows a high myoinositol peak, a moderately high choline peak, and a subtle reduction on the *N*-acetylaspartate peak (not shown). The diffusion tensor imaging–fractional anisotropy maps (*C–F*) and tractography (*G, H*) demonstrate that the main brain stem fiber tracts are preserved. This is probably explained by the fact that gliomatosis cerebri is a diffusely invading lesion that preserves the normal underlying cytoarchitectural pattern because it does not destroy the nerve fibers.

approaches. By examining the microscopic tissue environment, DTI may be able to delineate the tumor versus the infiltrating tumor between the peritumoral edema and normal brain parenchyma more accurately, which, in turn, may help to optimize the treatment of patients [69]. Although this remains to be proven, it does appear from straightforward inspection that DTI seems to be able to illustrate the relation of a tumor to the nearby main fiber tracts (Fig. 4). Because of this, many have begun to suggest that DTI might be used to aid in surgical planning [70] as well as radiotherapy planning [71] and to monitor tumor recurrence and the response to the treatment [72]. Examples of these applications are given below.

### *Tumor grading*

As mentioned previously, DWI (nontensor diffusion) seems to provide some utility in tumor grading by assessment of tumor cellularity. To

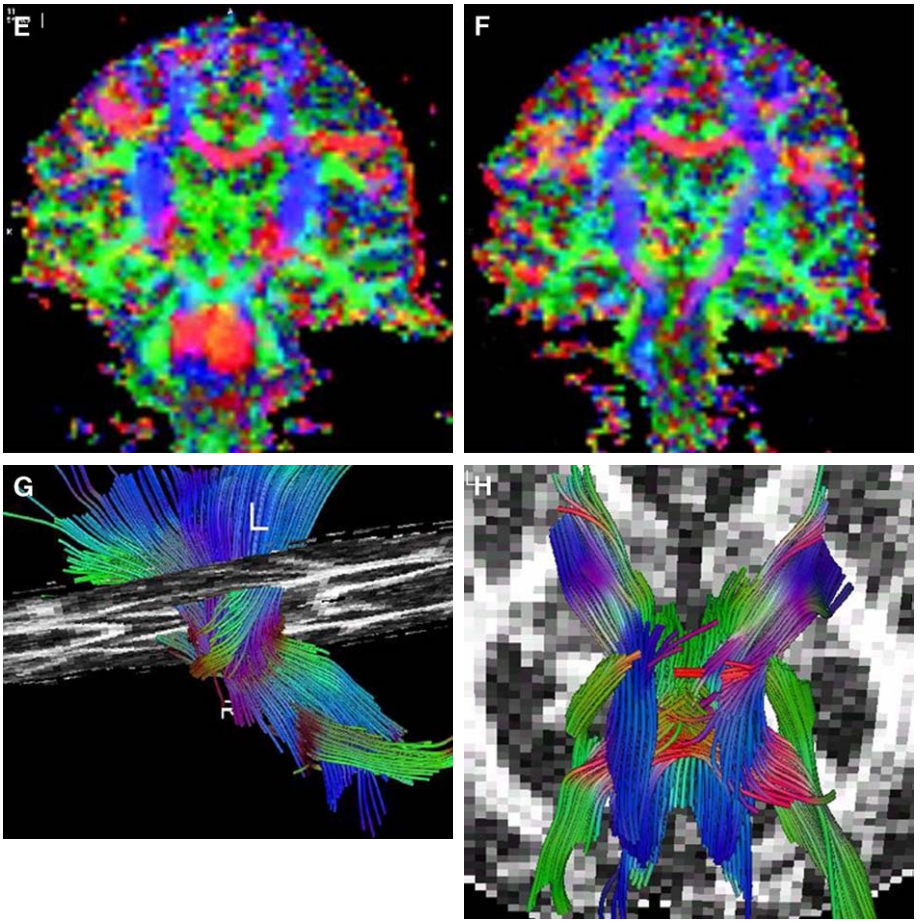


Fig. 6 (*continued*)

date, the additional information provided by DTI has not been shown to correlate with tumor cellularity [73], although in one series that evaluated epidermoid tumors with DTI, FA values were high, probably because of the high packing density of the cells and their solid-state cholesterol [74].

*Presurgical planning*

Much more enthusiasm has been shown for using DTI to illustrate the relation of a tumor to neighboring white matter tracts, with initial reports suggesting that this may be feasible [74]. DTI seems to be the only noninvasive method of obtaining information about the fiber tracts and is able to suggest them three dimensionally, although the validity of these suggestions remains to be studied carefully. Many practitioners accept an underlying assumption that the chief cause of anisotropy is related to the white matter bundles; with this assumption, the involvement of the white matter tracts can often be clearly identified in brain tumor patients by using anisotropic maps (the FA maps are the most widely used) and so-called "diffusion tractography," where images of the mathematically described connections between voxels are generated.

White matter involvement by a tumor can be arranged into five different categories as follows:

1. Displaced: maintained normal anisotropy relative to the contralateral tract in the corresponding location but situated in an abnormal T2-weighted signal intensity area or presenting in an abnormal orientation
2. Invaded: slightly reduced anisotropy without displacement of white matter architecture, remaining identifiable on orientation maps
3. Infiltrated: reduced anisotropy but remaining identifiable on orientation maps

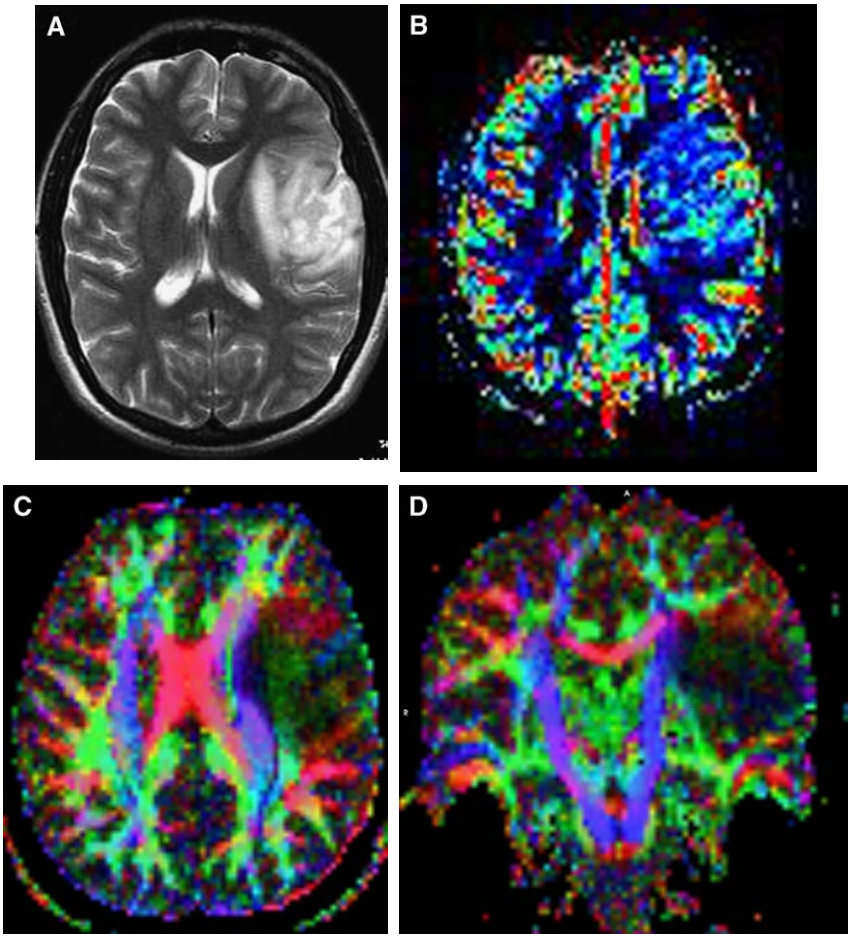


Fig. 7. A nonenhancing insular anaplastic astrocytoma lesion in a 56-year-old man (*A*), in which the relative cerebral blood volume map (*B*) demonstrates some areas of hyperperfusion within the lesion. There is infiltration of the corticospinal tract and corona radiata as well as of the superior longitudinal fasciculus on the axial (*C*) and coronal (*D, E*) diffusion tensor imaging (DTI)–fractional anisotropy maps and of the left corticospinal fibers tracts on tractography (*F*). DTI shows reduced anisotropy, but the main tracts remain identifiable on tractography.

4. Disrupted: marked reduced anisotropy and unidentifiable on orientation maps
5. Edematous: maintained normal anisotropy and normally oriented but located in an abnormal T2-weighted signal intensity area [75]

The neoplastic cells and the peritumoral edema cause changes in the brain structure; typically, measurement of diffusion anisotropy from the normal brain parenchyma up to near the tumor demonstrates a decrease in FA values [1].

Displacement rather than destruction of white matter fibers around low-grade gliomas has been described [71,76]. Low-grade neoplasms (Fig. 5) are well-circumscribed lesions that do not cause invasion or destruction of fiber tracts. These lesions tend to produce a deviation of surrounding white matter fibers. A study described a case in which the corticospinal tract (CST) had been infiltrated by an oligodendroglioma, although it spared the motor strip and the posterior limb of the internal capsule [77]. Displacement rather than infiltration of the adjacent white matter tracts has also been described in cerebral metastases [71] and meningiomas [78].

The main fiber tracts are invaded in cases of gliomatosis cerebri (Fig. 6), which has a specific histopathologic behavior. The neoplastic cells form parallel rows among nerve fibers, preserving

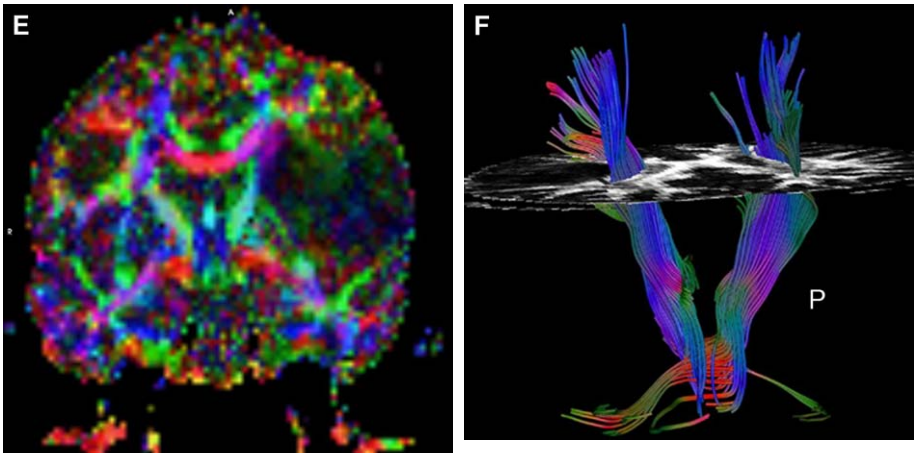


Fig. 7 (*continued*)

them; however, there is destruction of myelin sheaths. Thus, the anisotropy is slightly reduced when compared with normal subjects but greater than it is when compared with high-grade gliomas. The main fiber tracts remain identifiable on orientation maps and on the tractography.

The anisotropy in the T2-weighted hyperintense area that surrounds the tumor is reduced because of infiltration of neoplastic cells. Compared with the contralateral hemisphere in patients with high-grade gliomas (but not with low-grade gliomas or cerebral metastases) (Fig. 7), the anisotropy is also low in the white matter areas adjacent to tumors that look normal on T2-weighted images [71]. The same situation can be observed in lymphoma (Fig. 8). When compared with the abnormal white matter adjacent to metastases, Jellison et al [79] demonstrated decreased anisotropy of the abnormal white matter that surrounds the gliomas (Fig. 9). FA values decrease in the abnormal area that surrounds high-grade tumors on T2-weighted imaging. This presumably happens because of increased water content and tumor infiltration. A major brain structural disorganization then occurs [72]. Further study is necessary in this arena, because conflicting results have been described, with no difference found in FA value analyses of abnormal white matter adjacent to high-grade gliomas and metastases [72] in some studies.

The tract disruption mostly found in high-grade tumors (Fig. 10) may be caused by peritumoral edema, tumor mass effect, and tumor infiltration effect [71,78]. The anisotropic maps and tractography show destruction or discontinuation of the fiber tracts because of local tumor cell invasion (Fig. 11).

Metastatic lesions are surrounded by abnormal T2-weighted imaging that may consist of vasogenic edema. The edematous areas have reduced FA values. This fact can be explained by the increase in water content rather than by destruction or infiltration of nerve fibers. DTI did not help to differentiate apparently normal white matter from edematous brain and enhancing peritumoral margins [69]. The drop in FA values of the area infiltrated by cell tumors is lower than in the peritumoral edema [1,70,75]. DTI can distinguish the edematous areas with intact fibers mostly found in metastases (Fig. 12) from the disrupted fibers mostly found in high-grade gliomas [80].

In short, DTI is gaining support as a preoperative MRI method of evaluating brain tumors closely related to eloquent regions [75]. DTI seems to be particularly advantageous for certain types of surgical planning, optimizing the surgical evaluation of brain tumors near white matter tracts. Formal studies demonstrating that DTI can successfully prevent postoperative complications have yet to be performed, but preliminary data look promising [80].

### *Combination of diffusion tensor imaging with functional MRI*

Intracranial neoplasms may involve the functional cortex and the corresponding white matter tracts. The preoperative identification of eloquent areas through noninvasive methods, such as blood

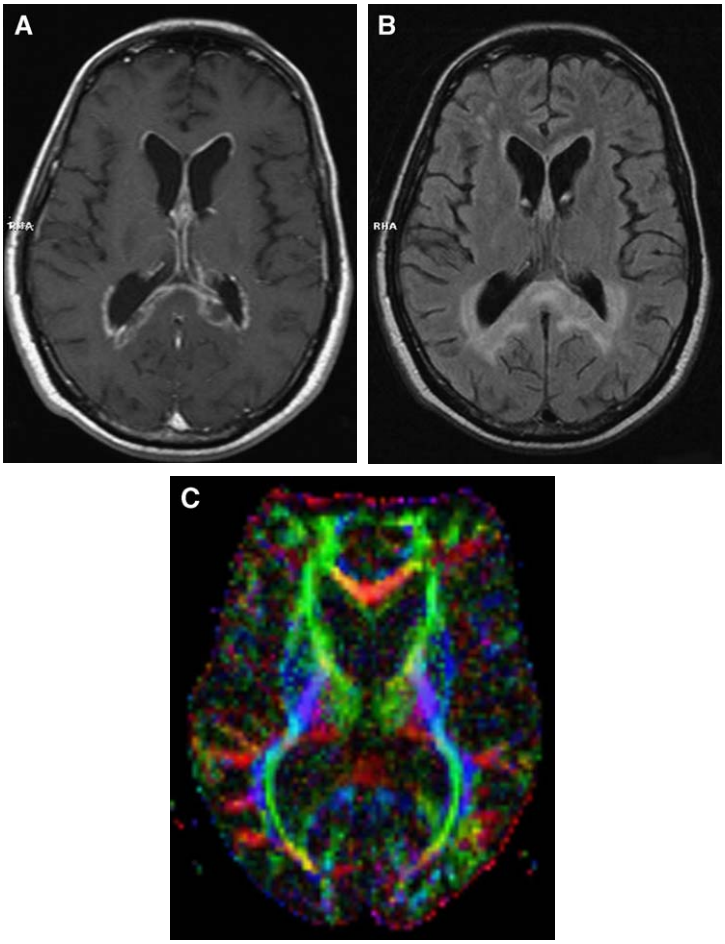


Fig. 8. A 50-year-old man with a histopathologic diagnosis of lymphoma complained of mental disturbance, cognitive impairment, and seizures. A contrast-enhanced, axial, T1-weighted image (*A*) demonstrates an enhancing lesion that involves the corpus callosum, surrounded by peritumoral edema/infiltrating lesion (*B*) associated with subependymal enhancement caused by cerebrospinal fluid dissemination. The axial fractional anisotropy color-coded map (*C*) demonstrates the infiltrating aspect of the lesion. The anisotropy in the splenium of the corpus callosum is markedly reduced.

oxygen level dependent (BOLD) fMRI and DTI tractography, offers some advantages; not only can it reduce the time of surgery in some instances, but it may minimize some intraoperative cortical stimulation methods, such as identification of the language cortex [80].

Until recently, preoperative and perioperative methods to evaluate brain function of patients with brain tumors were restricted to cortex activation. Increasingly, investigators are beginning to combine fMRI with DTI. The attraction is that fMRI can be an accurate and noninvasive method for mapping functional cerebral cortex, identifying eloquent areas in the cortex and displaying their relation to the lesion [81], whereas DTI may be able to identify the main fiber tracts to be avoided during surgery so as to safely guide a tumor resection [1]. Consequently, the combination of DTI tractography and fMRI might allow us to map an entire functional circuit precisely [82]. Even though fMRI locates eloquent cortical areas, determination of the course and integrity of the fiber tracts remains essential to the surgical planning [80,83].

This identification of the fiber tracts can facilitate the decision-making process regarding the likelihood of an operation [1]. As a result, neurosurgeons may have more information to

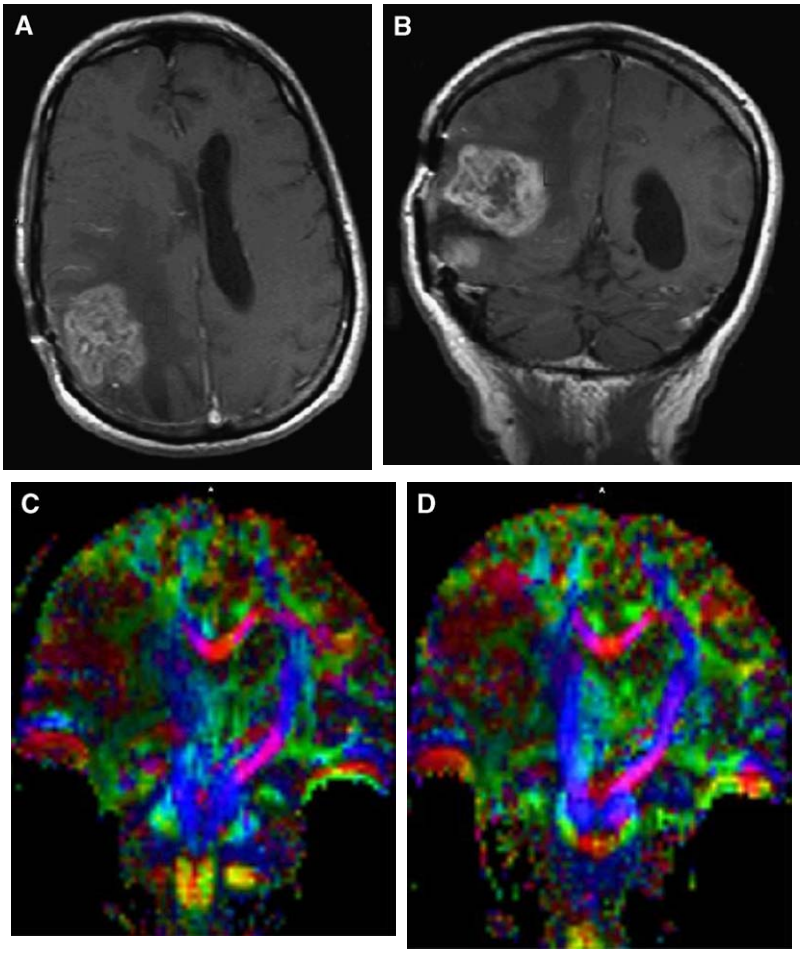


Fig. 9. (*A, B*) An expansive and infiltrating lesion in a 73-year-old man with left hemiparesis and seizures, with the diagnosis of glioblastoma multiforme. The lesion has hyperperfusion, markedly elevated choline and lactate/lipid peaks, and a low of *N*-acetylaspartate peak. (*C, D*) Coronal diffusion tensor imaging–fractional anisotropy maps show that the lesion dislocates and infiltrates the corticospinal tract and the superior longitudinal fasciculus. There is also distortion of the corpus callosum.

inform the choice of surgical approach to be taken. This better evaluation of risks by neurosurgeons is possible if they can know the spatial relation between the tumor and major fiber tracts [63] and thereby avoid postoperative neurologic deficit [2,83]. This remains to be proven in randomized trials, however.

Many investigators hope that the combined use of fMRI and DTI tractography might define the structural basis of functional connectivity in normal and pathologic brains [84]. As a consequence of the mass effect and changes in the structure of the brain caused by tumor, the identification of eloquent areas through conventional MRI results is, so to speak, impossible. Because fMRI is able to depict the exact location of the motor cortex in many instances, it should be possible to delineate the CST by DTI tractography. In one previous report [78], the authors used the motor cortex identified by fMRI as a starting point to trace the CST by DTI tractography. This approach could eventually be extended to other tracts as well.

The neurosurgical navigation system is a real-time device that provides a probe-guided intraoperative MRI (iMRI) display of the brain [85]. This system has already been widely used and is able to combine the information of fMRI [80,85] with that of DTI tractography [82,86], or even of both together [78,81].

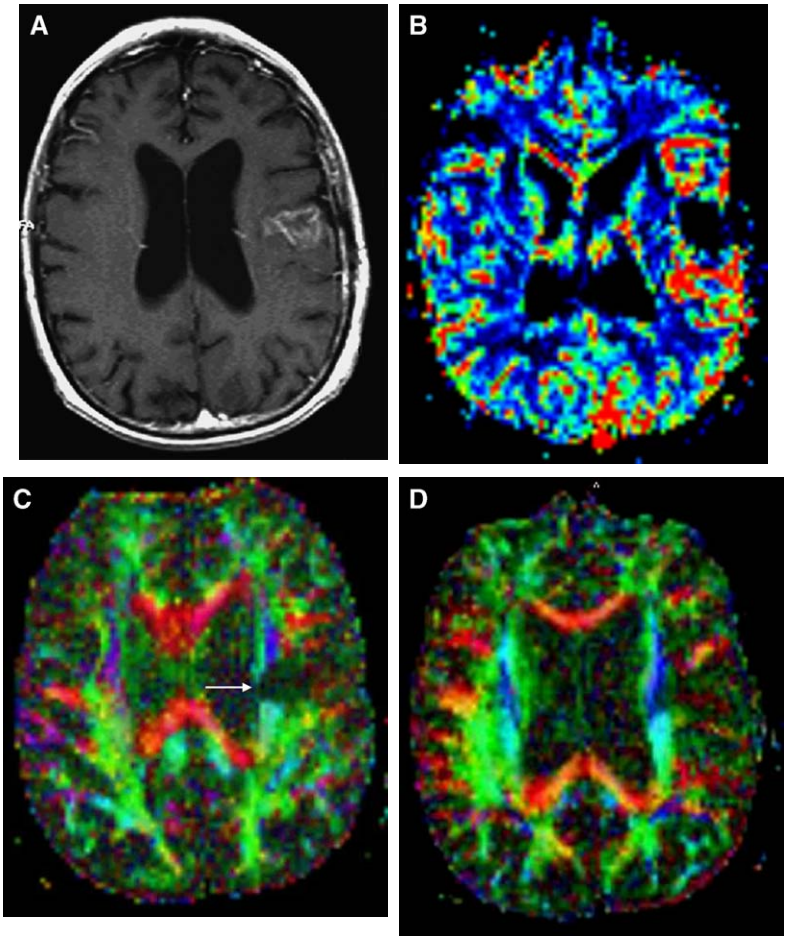


Fig. 10. A 56-year-old man with an anaplastic astrocytoma presented with right hemiparesis. The contrast-enhanced T1-weighted image (*A*) shows a left frontal lesion that has hyperperfusion on the relative cerebral blood volume map (*B*) (note the black signal caused by excessive enhancement with resulting T1 effect). (*C, D*) The axial diffusion-tensor imaging–fractional anisotropy maps demonstrate disruption of the left corona radiata (*arrow*).

*Intraoperative utility of diffusion tensor imaging*

iMRI has been used to guide a brain tumor resection. Such image-guidance systems can help to determine the optimal placement for the craniotomy.

Because surgical manipulations and maneuvers alter the anatomic position of brain structures and the tumor [87], morphologic changes of the brain may also occur between the time of the preoperative MRI examinations and the time of the surgery [88]. For this reason, the exact location of brain tumors based on preoperative examinations may not be the same. Because of this, iMRI has been proposed as a possible way to enable neurosurgeons to optimize their surgical approaches by avoiding critical structures and the adjacent normal brain parenchyma [87]. Some reports suggest that in 65% to 92% of the cases in which neurosurgeons believed they have performed a complete and thorough tumor resection, iMRI still depicts a lesion to be resected [89,90]. This is particularly relevant in low-grade gliomas, because studies suggest that total resection leads to a higher probability of cure. During surgery, however, such lesions can be difficult to differentiate from the normal brain parenchyma.

iMRI can be performed together with some functional sequences, such as fMRI [85] and diffusion imaging [82]. In one study, intraoperative diffusion imaging was performed during

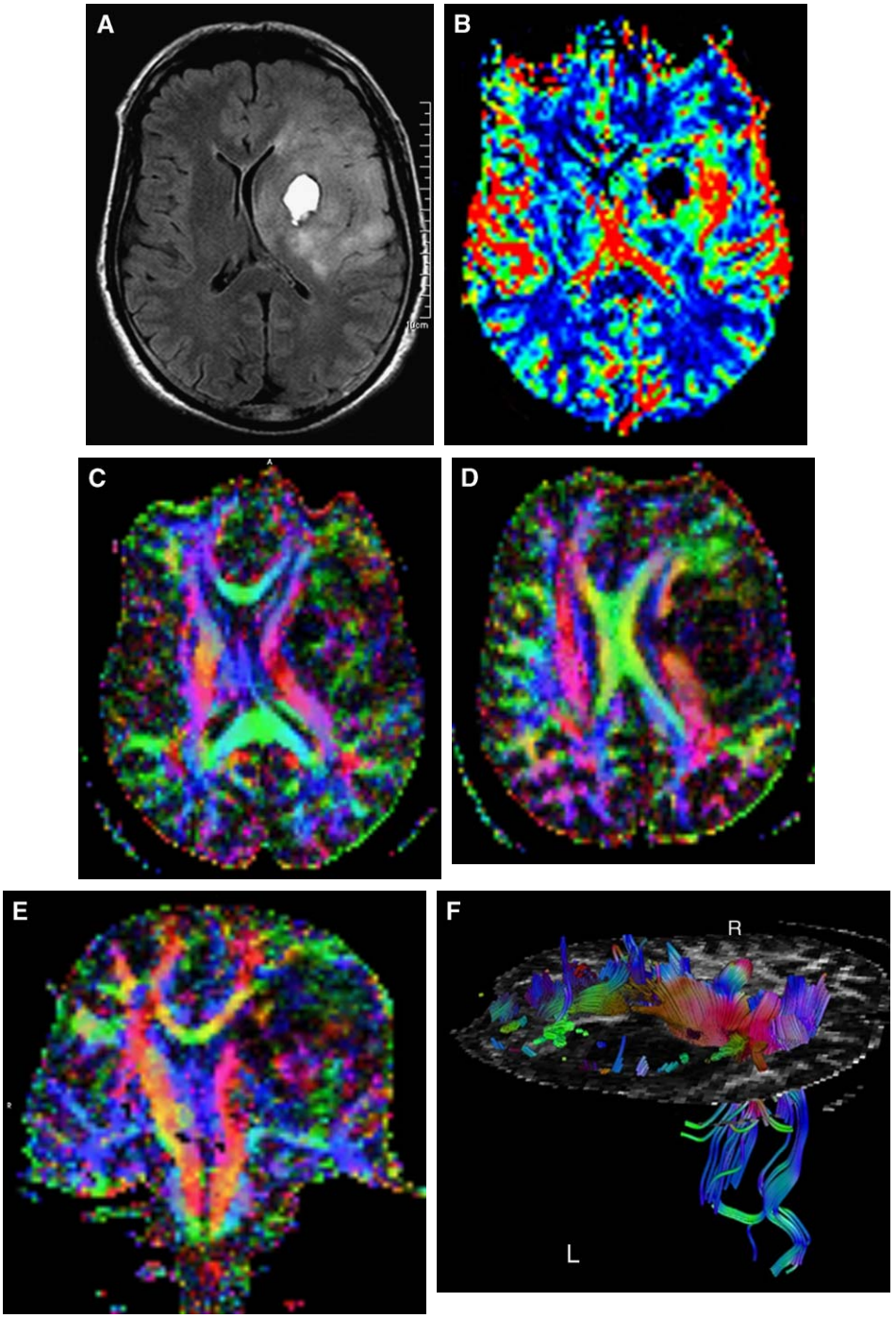


Fig. 11. A 57-year-old man with glioblastoma multiforme presented with right hemiparesis and seizures. An expansive, infiltrating, and enhancing left insular lesion with intratumoral hemorrhage (*A*) and hyperperfusion (*B*) is demonstrated. Axial (*C, D*) and coronal (*E*) diffusion tensor imaging–fractional anisotropy maps and tractography (*F*) show dislocation and disruption of the main fiber tracts, such as the anterior and posterior portions of the internal capsule and the superior longitudinal fasciculus.

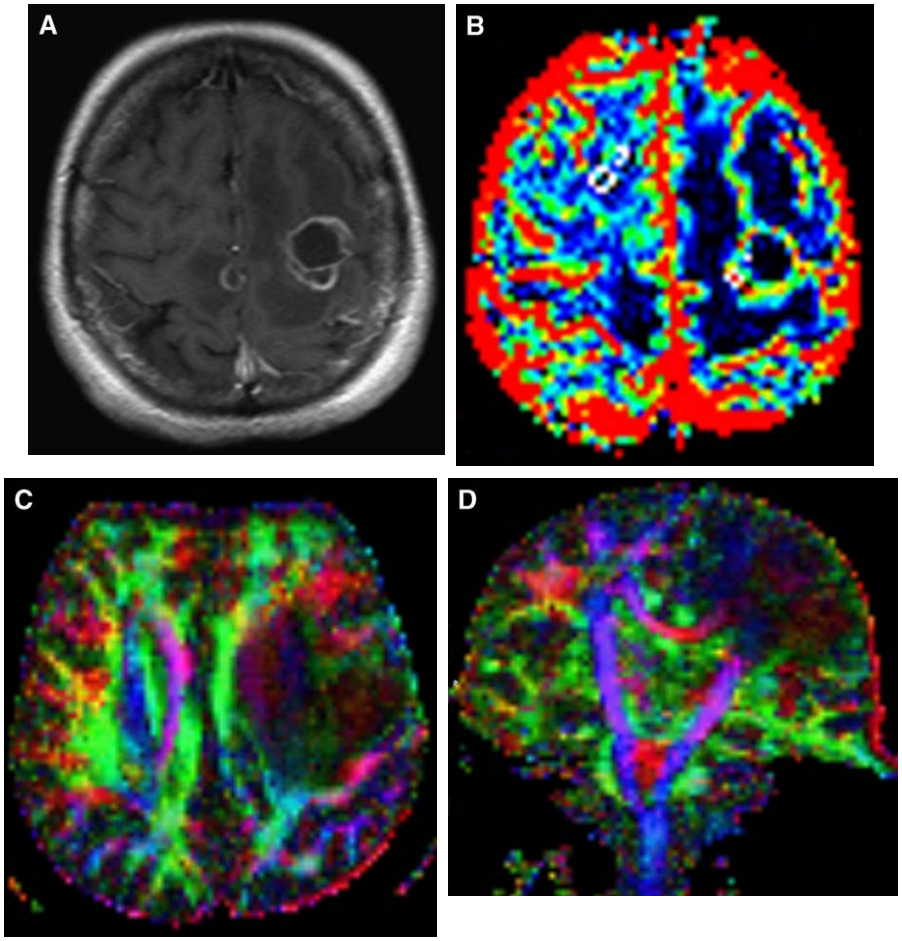


Fig. 12. A 50-year-old woman with new onset of seizures and a history of breast cancer. A round rim-enhancing lesion with a necrotic center (*A*) and hyperperfusion (*B*) is surrounded by peritumoral edema consisting of breast cancer metastasis. Axial (*C*) and coronal (*D*) diffusion tensor imaging–fractional anisotropy (FA) maps show the edematous changes in the FA values. Thus, it is difficult to identify the main fiber tracts within the vasogenic edema. This does not necessarily mean that these fibers are infiltrated with tumor or disrupted, however.

neurosurgery for the resection of a tumor using an interventional MRI system [82].

Intraoperative development of hyperacute cerebral ischemia had been previously detected in two patients, and this was confirmed later by a follow-up MRI examination. DTI, together with a neuronavigation system, was performed in a third patient as an integral part of an image-guided tumor resection. After processing the DTI data, DTI tractography was performed. The relation of the tumor to the anatomy of the white matter fiber tracts adjacent to it was clearly and plainly demonstrated in a case of oligodendroglioma. The fiber tracts were displaced, without being infiltrated or disrupted by the tumor. The complete tumor resection was performed without any postoperative neurologic deficit. Although anecdotal, such reports suggest that intraoperative diffusion imaging may provide important clinical information, adding substantially to the intraoperative information available about the pathologic state of the brain parenchyma and the structure of white matter.

### *Diffusion tensor imaging in brain tumor therapy*

DTI may play a role in the management of patients undergoing radiation therapy and chemotherapy. By adding information about the location of white matter tracts, DTI tractography

might be used successfully alongside fMRI for radiosurgery planning. In theory, this should allow a reduction of the dose applied as well as a reduction in the volume of normal brain irradiated with a high dose, hopefully reducing necrosis [71].

DTI may also help in the early detection of white matter injuries caused by chemotherapy and radiation therapy. A report showed a correlation between the reduction of FA values, young age at treatment, an increased interval since the beginning of treatment, and the poor intellectual outcome in patients with medulloblastoma [91]. The possibility of using FA or other DTI changes as a biomarker for neurotoxicity is enticing.

## Limitations

Although initial reports suggest advantages of DTI in the evaluation of patients with brain tumors, these reports are largely single-center, uncontrolled, preliminary findings. Therefore, these results must be cautiously interpreted. Furthermore, there remain substantial technical hurdles, with the rapid evolution of MRI systems making ever more powerful approaches possible. Such improvements are particularly welcome, given the limited signal-to-noise ratio of diffusion overall. For example, the limited spatial resolution of EPI approaches may lead to reduced sensitivity. The method herein assessed is only capable of depicting the prominent fiber tracts [70,92], and more advanced approaches (eg, diffusion spectrum imaging) may be much more useful in the future. Susceptibility artifacts can cause image distortion that prevents DTI data from being accurately analyzed [70], and numerous other technical challenges remain. Nevertheless, these initial data are promising.

## Summary

DTI seems to offer the possibility of adding important information to presurgical planning. Although experience is limited, DTI seems to provide useful local information about the structures near the tumor, and this seems to be useful in planning. In the future, DTI may provide an improved way to monitor intraoperative surgical procedures as well as their complications. Furthermore, evaluation of the response to treatment with chemotherapy and radiation therapy might also be possible. Although DTI has some limitations, its active investigation and further study are clearly warranted.

## References

[1] Landis SH, Murray T, Bolden S. Cancer statistics, 1998. CA Cancer J Clin 1998;48:6–29.
[2] Berens ME, Rutka JT, Rosenblum ML. Brain tumor epidemiology, growth, and invasion. Neurosurg Clin N Am 1990;1:1–18.
[3] Koeller KK, Henry JM. Superficial gliomas: radiologic-pathologic correlation. Radiographics 2001; 21:1533–56.
[4] Hunt D, Treasure P. Year of life lost due to cancer in East Anglia 1990–1994. Cambridge: East Anglian Cancer Intelligence Unit, Institute of Public Health; 1998.
[5] Brain MRC Tumor Working Party. Prognostic factor for high-grade malignant glioma: development of a prognostic index. A report of the Medical Research Council Brain Tumor Working Party. J Neurooncol 1990;9:47–55.
[6] Damadian R. Tumor detection by nuclear magnetic resonance. Science 1971;171:1151–3.
[7] Tovi M. MR imaging in cerebral gliomas analysis of tumor tissue components. Acta Radiol Suppl 1993; 384:1–24.
[8] Brunberg JA, Chenevert TL, McKeever PE, Ross DA, Junck LR, Muraszko KM, et al. In vivo MR determination of water diffusion coefficients and diffusion anisotropy: correlation with structural alteration in gliomas of the cerebral hemispheres. AJNR Am J Neuroradiol 1995;16:361–71.
[9] Tien RD, Felsberg GJ, Friedman H, Brown M, MacFall J. MR imaging of high-grade cerebral gliomas: value of diffusion-weighted echo-planar pulse sequence. AJR Am J Roentgenol 1994;162:671–7.
[10] Holodny AI, Ollenschlager M. Diffusion imaging in brain tumor. Neuroimaging Clin N Am 2002;12: 107–24.
[11] Le Bihan D, Breton E, Lallemand D, Aubin MI, Vignaud J, Laval-Jeantet M. Diffusion and perfusion in intravoxel incoherent motion MR imaging. Radiology 1988;168:497–505.
[12] Turner R, Le Bihan D, Maier J, Vavrek R, Hedges LK, Pekar J. Echo-planar imaging of intravoxel incoherent motion. Radiology 1990;177: 407–14.
[13] Barboriak DP. Imaging of brain tumors with diffusion-weighted and diffusion tensor MR imaging. Magn Reson Imaging Clin N Am 2003;11:379–401.
[14] Maier SE, Gudbjartsson H, Patz SL, Hsu L, Lovblad KO, Edelman RR, et al. Line scan diffusion imaging: characterization in healthy subjects and stroke patients. AJR Am J Roentgenol 1998;171: 85–93.
[15] Warach S, Chien D, Li W, Ronthal M, Edelman RR. Fast magnetic resonance diffusion-

weighted imaging of acute human stroke. Neurology 1992;42:1717–23.
[16] Sunshine JL, Tarr RW, Lanzieri CF, Landis DM, Selman WR, Lewin JS. Hyperacute stroke: ultrafast MR imaging to triage patients prior to therapy. Radiology 1999;212:325–32.
[17] Beauchamp NJ, Uluğ AM, Passe TJ, van Zijl PC. MR diffusion imaging in stoke: review and controversies. Radiographics 1998;18:1269–83.
[18] Schaefer PW. Applications of DWI in clinical neurology. J Neurol Sci 2001;186(Suppl 1):S25–35.
[19] Larsson HB, Thomsen C, Frederiksen J, Stubgaard M, Henriksen O. In vivo magnetic resonance measurement in the brain of patients with multiple sclerosis. Magn Reson Imaging 1993;10:7–12.
[20] Horsfield MA, Lai M, Webb SL, Barker GJ, Tofts PS, Turner R, et al. Apparent diffusion coefficients in benign and secondary progressive multiple sclerosis by nuclear magnetic resonance. Magn Reson Med 1996;36:393–400.
[21] Castriota-Scanderberg A, Tomaiuolo F, Sabatini U, Nocentini U, Grasso MG, Caltagirone C. Demyelinating plaques in relapsing-remitting and secondary progressive multiple sclerosis: assessment with diffusion MR imaging. AJNR Am J Neuroradiol 2000; 21:862–8.
[22] Tsuchiya K, Hachiya J, Maehara T. Diffusion-weighted MR imaging in multiple sclerosis: comparison with contrast-enhanced study. Eur J Radiol 1999;10:7–12.
[23] Tsuchiya K, Katase S, Yoshino A, Hachiya J. Diffusion-weighted MR imaging of encephalitis. AJR Am J Roentgenol 1999;173:1097–9.
[24] Na DL, Suh CK, Choi SH, Moon HS, Seo DW, Kim SE, et al. Diffusion-weighted magnetic resonance imaging in probable Creutzfeldt-Jakob disease. Arch Neurol 1999;56:951–7.
[25] Stejskal E, Tanner J. Spin diffusion measurements: spin echos in the presence of time-dependent field gradient. J Chem Phys 1965;42:288–92.
[26] Romero JM, Schaefer PW, Grant PE, Becerra L, Gonzáles RG. Diffusion MR imaging of acute ischemic stroke. Neuroimaging Clin N Am 2002;12: 35–53.
[27] Eis M, Els T, Hoehn-Berlage M, Hossman KA. Quantitative diffusion MR imaging of cerebral tumor and edema. Acta Neurochir Suppl (Wien) 1994;60:344–6.
[28] Krabbe K, Gideon P, Wang P, Hansen U, Thomsen C, Madsen F. MR diffusion imaging of human intracranial tumours. Neuroradiology 1997; 39:483–9.
[29] Le Bihan D, Douek P, Argyropoulou M, Turner R, Patronas N, Fulham M. Diffusion and perfusion magnetic resonance imaging in brain tumors. Top Magn Reson Imaging 1993;5:25–31.
[30] Tsuruda JS, Chew WM, Moseley ME, Norman D. Diffusion-weighted MR imaging of extraaxial tumors. Magn Reson Med 1991;19:316–20.
[31] Yanaka K, Shirai S, Kimura H, Kamezaki T, Matsumura A, Nose T. Clinical application of diffusion-weighted magnetic resonance imaging to intracranial disorders. Neurol Med Chir 1995;16:361–71.
[32] Guo AC, Provenzale JM, Cruz LCH Jr, Petrella JR. Cerebral abscesses: investigation using apparent diffusion coefficient maps. Neuroradiology 2001;43: 370–4.
[33] Bergui M, Zhong J, Bradac GB, Sales S. Diffusion-weighted images of intracranial cyst-like lesions. Neuroradiology 2001;439(10):824–9.
[34] Chang SC, Lai PH, Chen WL, Weng HH, Ho JT, Wang JS. Diffusion-weighted MRI features of brain abscess and cystic or necrotic brain tumors: comparison with conventional MRI. Clin Imaging 2002; 26(4):227–36.
[35] Chan JH, Tsui EY, Chau LF, Chow KY, Chan MS, Yuen MK, et al. Discrimination of an infected brain tumor from a cerebral abscess by combined MR perfusion and diffusion imaging. Comput Med Imaging Graph 2002;26(1):19–23.
[36] Ebisu T, Tanaka C, Umeda M, Kitamura M, Naruse S, Higuichi T, et al. Discrimination of brain abscess from necrotic or cystic tumors by diffusion-weighted echo planar imaging. Magn Reson Imaging 1996;14(9):1113–6.
[37] Hartmann M, Jansen O, Heiland S, Sommer C, Munkel K, Sartor K. Restricted diffusion within ring enhancement is not pathognomonic for brain abscess. AJNR Am J Neuroradiol 2001;22(9):1738–42.
[38] Tsuruda JS, Chew WM, Moseley ME, Norman D. Diffusion-weighted MR imaging of the brain: value of differentiating between extra-axial cysts and epidermoid tumors. AJNR Am J Neuroradiol 1990; 155:1049–65.
[39] Chen S, Ikawa F, Kurisu K, Arita K, Takaba J, Kanou Y. Quantitative MR evaluation of intracranial epidermoid tumors by fast fluid-attenuated inversion recovery imaging and echo-planar diffusion-weighted imaging. AJNR Am J Neuroradiol 2001;22(6):1089–96.
[40] Laing AD, Mitchell PJ, Wallace D. Diffusion-weighted magnetic resonance imaging of intracranial epidermoid tumors. Aust Radiol 1999;43:16–9.
[41] Burger PC, Heinz ER, Shibata T, Kleihues P. Topographic anatomy and CT correlations in the untreated glioblastoma multiforme. J Neurosurg 1988; 68:698–704.
[42] Johnson PC, Hunt SJ, Drayer BP. Human cerebral gliomas: correlation of postmortem MR imaging and neuropathologic findings. Radiology 1989;170: 211–7.
[43] Yoshiura T, Wu O, Zaheer A, Reese TG, Sorensen AG. Highly diffusion-sensitized MRI of brain: dissociation of gray and white matter. Magn Reson Med 2001;45:734–40.
[44] Stadnik TW, Chaskis C, Michotte A, Shabana WM, van Rompaey K, Luypaert R, et al. Diffusion-weighted MR imaging of intracerebral masses:

comparison with conventional MR imaging and histologic findings. AJNR Am J Neuroradiol 2001;22: 969–76.

[45] Castillo M, Smith JK, Kwock L, Wilber K. Apparent diffusion coefficients in the evaluation of high-grade cerebral gliomas. AJNR J Neuroradiol 2001; 22(1):60–4.

[46] Kono K, Inoue Y, Nakayama K, Shakudo M, Morino M, Ohata K, et al. The role of diffusion-weighted imaging in patients with brain tumors. AJNR Am J Neuroradiol 2001;22:1081–8.

[47] Sugahara T, Korogi Y, Kochi M, Ikushima I, Shigematu Y, Hirai T, et al. Usefulness of diffusion-weighted MRI with echo-planar technique in the evaluation of cellularity in gliomas. J Magn Reson Imaging 1999;9:53–60.

[48] Noguchi K, Watanabe N, Nagayoshi T, Kanazawa T, Toyoshima S, Shimizu M, et al. Role of diffusion-weighted echo-planar MRI in distinguishing between brain abscess and tumor: a preliminary report. Neuroradiology 1999;41:171–4.

[49] Guo AC, Cummings TJ, Dash RC, Provenzale JM. Lymphomas and high-grade astrocytomas: comparison of water diffusibility and histologic characteristics. Radiology 2002;224(1):177–83.

[50] Singh S, Leeds N. Postoperative diffusion imaging in the setting of craniotomies for brain masses: incidence of ischemia. Presented at the American Society of Neuroradiology 40th Annual Meeting. Vancouver, May 10–12, 2002.

[51] Kauppienen RA. Monitoring cytotoxic tumour treatment response by diffusion magnetic resonance imaging and proton spectroscopy. NMR Biomed 2002;15(1):6–17.

[52] Chenevert TL, Stegman LD, Taylor JM, Robertson PL, Greenberg HS, Rehemtulla A, et al. Diffusion magnetic resonance imaging: an early surrogate marker of therapeutic efficacy in brain tumors. J Natl Cancer Inst 2000;92(24): 2029–36.

[53] Valk PE, Dillon WP. Radiation injury of the brain. AJNR Am J Neuroradiol 1991;12(1):45–62.

[54] Fujikawa A, Tsuchiya K, Katase S, Kurosaki Y, Hachiya J. Diffusion-weighted MR imaging of carmofur-induced leukoencephalopathy. Eur Radiol 2001;11(12):2602–6.

[55] Chenevert TL, Brunberg JA, Pipe JG. Anisotropic diffusion in human white matter: demonstration with MR techniques in vivo. Radiology 1990;177: 401–5.

[56] Moseley ME, Cohen Y, Kucharczyk J, Mintorovitch J, Asgari HS, Wendland. Diffusion-weighted MF. MR imaging of anisotropic water diffusion in cat central nervous system. Radiology 1990;176:439–45.

[57] Melhem ER, Mori S, Mukundan G, Kraut MA, Pomper MG, Van Zijl PCM. Diffusion tensor MR imaging of the brain and white matter tractography. AJR Am J Roentgenol 2002;178(1):3–16.

[58] Ito R, Mori S, Melhem ER. Diffusion tensor MR imaging and tractography. Neuroimaging Clin N Am 2002;12(1):1–19.

[59] Pierpaoli C, Jezzard P, Basser P, Barnett A, Di Chiro G. Diffusion tensor MR imaging of the human brain. Radiology 1996;201:637–48.

[60] Basser PJ, Mattiello J, LeBihan D. Estimation of the effective self-diffusion tensor from the NMR spin echo. J Magn Reson B 1994;103:247–54.

[61] Shimony JS, McKinstry RC, Akbudak E, Aranovitz JA, Snyder AZ, Lori NF, et al. Quantitative diffusion-tensor anisotropy brain MR imaging: normative human data and anatomic analysis. Radiology 1999;212:770–84.

[62] Basser PJ, Pajevic S, Pierpaoli C, Duda J, Aldroubi A. In vivo fiber tractography using DT-MRI data. Magn Reson Med 2000;44:625–32.

[63] Mamata H, Mamata Y, Westin CF, Shenton ME, Kikinis R, Jolesz FA, et al. High-resolution line scan diffusion tensor MR imaging of white matter fiber tract anatomy. AJNR Am J Neuroradiol 2002;23: 67–75.

[64] Douek P, Turner R, Pekar J, Patronas N, Le Bihan D. MR color mapping of myelin fiber orientation. J Comput Assist Tomogr 1991;15(6):923–9.

[65] Pajevic S, Pierpaoli C. Color schemes to represent the orientation of anisotropic tissues from diffusion tensor data: application to white matter fiber tract mapping in the human brain. Magn Reson Med 1999;42:526–40.

[66] Maldjian JA, Schulder M, Liu WC, Mun IK, Hirschorn D, Murthy R, et al. Intraoperative functional MRI using a real-time neurosurgical navigation system. J Comput Assist Tomogr 1997;21: 910–2.

[67] Schulder M, Maldjian JA, Liu WC, Holodny AI, Kalnin AT, Mun IK, et al. Functional image-guided surgery of intracranial tumors located in or near the sensorimotor cortex. J Neurosurg 1998;89:412–8.

[68] Tovi M. MR imaging in cerebral gliomas analysis of tumor tissue components. Acta Radiol Suppl 1993; 384:1–24.

[69] Sha S, Bastin ME, Whittle IR, Wardlaw JM. Diffusion tensor MR imaging of high-grade cerebral gliomas. AJNR Am J Neuroradiol 2002;23: 520–7.

[70] Mori S, Frederiksen K, Van Zijl PCM, Stieltjes B, Kraut MA, Slaiyappan M, et al. Brain white matter anatomy of tumor patients evaluated with diffusion tensor imaging. Ann Neurol 2002;51:377–80.

[71] Price SJ, Burnet NG, Donovan T, Green HAL, Pena A, Antoun NM, et al. Diffusion tensor imaging of brain tumors at 3T: a potential tool for assessing white matter tract invasion. Clin Radiol 2003;58: 455–62.

[72] Lu S, Ahn D, Johnson G, Cha S. Peritumoral diffusion tensor imaging of high-grade gliomas and metastatic brain tumors. AJNR Am J Neuroradiol 2003;24:937–41.

[73] Gauvain KM, McKinstry RC, Mukherjee P, Perry A, Neil JJ, Kaufman BA, et al. Evaluating pediatric brain tumor cellularity with diffusion-tensor imaging. AJR Am J Roentgenol 2001;177:449–54.
[74] Koot RW, Jagtab AP, Akkerman EM, Heeten GJD, Majoie CBLM. Epidermoid of the lateral ventricle: evaluation with diffusion-weighted and diffusion tensor imaging. Clin Neurol Neurosurg 2003;105: 270–3.
[75] Witwer BP, Moftakhar R, Hasan KM, Deshmukh P, Haughton V, Field A, et al. Diffusion-tensor imaging of white matter tracts in patients with cerebral neoplasm. J Neurosurg 2002;97:568–75.
[76] Weishmann UC, Symms MR, Parker GJM, Clark CA, Lemieux L, Barker GJ, et al. Diffusion tensor imaging demonstrates deviation of fibers in normal appearing white matter adjacent to a brain tumour. J Neurol Neurosurg Psychiatry 2000;68: 501–3.
[77] Holodny AI, Schwartz TH, Ollenschleger M, Liu WC, Schulder M. Tumor involvement of the corticospinal tract: diffusion magnetic resonance tractography with intraoperative correlation. J Neurosurg 2001;95(6):1082.
[78] Holodny AI, Ollenschleger M, Liu WC, Schulder M, Kalnin AJ. Identification of the corticospinal tracts achieved using blood-oxygen-level-dependent and diffusion functional MR imaging in patients with brain tumors. Am J Neuroradiol 2001;22:83–8.
[79] Jellison NJ, Wu Y, Field AS, Hasan KM, Alexander AL, Badie B. Diffusion tensor imaging metrics for tissue characterization: discriminating vasogenic edema from infiltrating tumor. Presented at the American Society of Neuroradiology 41st Annual Meeting. Washington, DC, April 27–May 1, 2003.
[80] Tummala RP, Chu RM, Liu H, Truwit C, Hall WA. Application of diffusion-tensor imaging to magnetic-resonance-guided brain tumor resection. Pediatr Neurosurg 2003;39:39–43.
[81] Schulder M, Maldjian JA, Liu W-C, Holodny AI, Kalnin AT, Mun IK, et al. Functional image-guided survey of intracranial tumors located in or near the sensorimotor cortex. J Neurosurg 1998;89:412–8.
[82] Krings T, Reiges MH, Thiex R, Gilsbach JM, Thron A. Functional and diffusion-weighted magnetic resonance images of space-occupying lesions affecting the motor system: imaging the motor cortex and pyramidal tracts. J Neurosurg 2001;95(5): 816–24.
[83] Mamata Y, Mamata H, Nabavi A, Kacher DF, Pegolizzi RS Jr, Schwartz RB, et al. Intraoperative diffusion imaging on a 0.5 Tesla interventional scanner. J Magn Reson Imaging 2001;13:115–9.
[84] Guye M, Parker GJM, Symms M, Boulby P, Wheeler-Kingshott CAM, Salek-Haddadi A, et al. Combined functional MRI and tractography to demonstrate the connectivity of the human primary motor cortex in vivo. Neuroimage 2003;19: 1349–60.
[85] Maldjian JA, Schulder M, Liu W-C, Mun I-K, Hirschorn D, Murthy R, et al. Intraoperative functional MRI using a real-time neurosurgical navigation system. J Comput Assist Tomogr 1997;21(6): 910–2.
[86] Krings T, Coenen VA, Axer H, Reinges MHT, Holler M, von Keyserlingk DG, et al. In vivo 3D visualization of normal pyramidal tracts in human subjects using diffusion weighted magnetic resonance imaging and a neuronavigator system. Neurosci Lett 2001;307:192–6.
[87] Jolesz FA, Talos I-F, Schwartz RB, Mamat H, Kacher DF, Hynynen K, et al. Intraoperative magnetic resonance imaging and magnetic resonance imaging-guided therapy of brain tumors. Neuroimaging Clin N Am 2002;12:665–83.
[88] Martin AJ, Hall WA, Liu H, Pozza CH, Michel E, Casey SO, et al. Brain tumor resection: intraoperative monitoring with high-field-strength MR imaging—initial results. Radiology 2000;215:221–8.
[89] Bradley WG. Achieving gross total resection of brain tumors: intraoperative MR imaging can make a big difference. AJNR Am J Neuroradiol 2002;23: 348–9.
[90] Albert FK, Forsting M, Sartor K, Adams HP, Kunze S. Early post-operative magnetic resonance imaging after resection of malignant glioma: objective evaluation of residual tumor growth and its influence on regrowth and prognosis. Neurosurgery 1994;34:45–61.
[91] Khong P-L, Kwong DL, Chan GCF, Sham JST, Cham F-L, Ooi G-C. Diffusion-tensor imaging for the detection and qualification of treatment-induced white matter injury in children with medulloblastoma: a pilot study. AJNR Am J Neuroradiol 2003;24:734–40.
[92] Yamada K, Kizu O, Mori S, Ito H, Nakamura H, Yuen S, et al. Brain fibertracking with clinically feasible diffusion-tensor MR imaging: initial experience. Radiology 2003;227:295–301.